A novel mechanism controls Li mineralization in granitic pegmatite

Xin Zhang (zhangxin869@nxu.edu.cn)
Ningxia University
Hui Zhang
Chinese Academy of Sciences
Yong Tang
Chinese Academy of Sciences
Zheng-Hang Lv
Chinese Academy of Sciences
Shen-Jin Guan
Kunming University of Science and Technology
Meng-Tao Wang
Chinese Academy of Sciences

Article

Keywords: Mechanism of Li mineralization, granitic pegmatite, Li isotope, fluid exsolution

Posted Date: April 4th, 2022

DOI: https://doi.org/10.21203/rs.3.rs-1508012/v1

A novel mechanism controls Li mineralization in granitic pegmatite

Xin Zhang[1*], Hui Zhang[2*], Yong Tang[2], Zheng-Hang Lv[2], Shen-Jin Guan[3], Meng-Tao Wang[2]

[1]School of Geography and Planning, Ningxia University, Yinchuan 750021, PR China

[2]Key Laboratory of High-Temperature and High-Pressure Study of the Earth's Interior, Institute of Geochemistry, Chinese Academy of Sciences, Guiyang 550002, PR China

[3]Faculty of Land Resources Engineering, Kunming University of Science and Technology, Kunming 650093, PR China

[*]Corresponding authors

Correspondence and requests for materials should be addressed to Xin Zhang (email: zhangxin869@nxu.edu.cn)

Abstract

Granitic pegmatite Li deposits account for approximately half of global Li production, while the Li mineralization mechanism remains enigmatic. Here we present Li isotope data on the albite from 8 textural zones of the well-characterized Koktokay No. 3 Li-Be-Nb-Ta-Rb-Cs mineralized pegmatite in Xinjiang, China. Our results reveal that there coexists two important processes during the internal evolution of the pegmatite: (1) fluid exsolution and (2) Li unloading. The former facilitates Li enrichment and the later results in spodumene crystallization. These "fluid transportation" processes can be indicated by a negative correlation between δ^7Li value and Li content. Globally, the statistical geochemical data of Li mineralized pegmatites have also yielded a negative linear correlation between δ^7Li value and Li content in both of whole rock and separated mineral samples, providing compelling evidence that "fluid transportation" is the key mechanism responsible for Li mineralization in granitic pegmatites. This finding is of great significance for Li metal deposit modeling, highlighting an urgent need to better understand the dynamic processes of magmatic-hydrothermal interaction during the crystallization of pegmatite magma.

Keywords

Mechanism of Li mineralization, granitic pegmatite, Li isotope, fluid exsolution

Introduction

Lithium metal is in high demand because of recent technological advances have made it an indispensable raw material in the nuclear, electronic, optical, ceramic, and glass industries[1]. Granitic pegmatite is essentially an igneous rock characterized by extremely coarse but variable grain size[2,3]. This rock is commonly enriched in incompatible lithophile elements and thus has been considered as an important economic source of Li rare metal[4].

Finding the mechanism responsible for Li mineralization in granitic pegmatite is essential for Li metal deposit modeling and mineral exploitation, and this issue has prompted a long-standing scientific discussion. Experimental studies from Webster et al.[5] revealed that the distribution coefficients of rare-metal elements between aqueous fluids and melts of topaz rhyolite composition increase as the Cl concentration of the fluid increases, indicating that rare-metal elements may become differentiated as potentially facilitated by the movement of Cl-rich aqueous fluids. Later, Shearer et al.[6] argued that moderate to high degrees fractional crystallization (up to 70~90%) of volatile-rich magmas can produce extreme rare-element enrichments in pegmatites on the basis of a case study of the Harney Peak granite-pegmatite system in the Black Hills. Veksler et al.[7] found experimental evidence of three coexisting immiscible fluids in synthetic granitic pegmatite and suggested that hydrosaline melts can be effective agents for enhanced ore formation in pegmatites. More recently, London[3] proposed that constitutional zone refining via the creation of a boundary layer liquid, chemically distinct from but continuous with the bulk melt at the crystallization front, may be the key mechanism controlling rare-metal elements enrichment during the evolution of pegmatite magma. While, Thomas and Davidson[8] considered that there exists supercritical silicate melt/fluid in the evolution of pemgatite magmas and emphasized its important role that plays in rare-metal elements enrichment.

The characteristic textural development and internal mineral-assemblage zoning of granitic pegmatite are generally ascribed to the effects of non-granitic components that act as fluxes in the melt or in the separate fluid[9], or to the effects of liquidus undercooling of granitic melts[10]. Several experimental studies have successfully reproduced the pegmatite textures[11–14]. It is interesting that in well-evolved zoning granitic pegmatites Li mineralization usually occurs in the intermediate

zones, but not in the border zone, wall zone or core zone[3,4,15], such as the Koktokay No. 3 pegmatite in China[16,17], the Tanco pegmatite in Canada[18,19] and the Bikita pegmatite in Zimbabwe[20]. These indicate that key mechanism controlling Li accumulation and mineralization lies in the crystallization processes of pegmatite magma. Thus, a systematic investigation into the migration of Li through the whole internal evolutionary processes of a granitic pegmatite may provide new clues.

Lithium has two stable isotopes, ^{6}Li and ^{7}Li. The large mass difference (~15%) between these two isotopes produces large isotopic fractionation especially during low-temperature alteration[21], chemical diffusion[22] and fluid interaction[23]. For these reasons, Li isotope can be employed as a sensitive indicator for precisely tracking the processes related to Li migration. The Koktokay No. 3 pegmatite (Figure 1) is the largest Li-Be-Nb-Ta-Rb-Cs rare-metal deposit in the Altay orogenic belt, and is world-famous for its complete and highly-differentiated internal mineral-assemblage zoning[16,17]. Here we present Li isotopic and trace elemental data on the albite from 8 textural zones of this pegmatite, with suitable precision to identify possible mechanism for Li mineralization.

Results and discussion

Li isotopic compositions of sample

Albite is the most important rock-forming mineral in granitic pegmatite[3,4], and Li isotopic fractionation between alkali feldspar and pegmatite is negligible[24] ($\Delta Li_{Afs-pegmatite} < 0.6‰$). Thus, $\delta^{7}Li$ of albite in different textural zones can help to constrain the chemical evolution of pegmatite magma. The Li isotopic and elemental data of samples are given in Table S1, Table S2 and Table S3. The $\delta^{7}Li$ has a broad range of 0.55–11.15‰ and so we are able to document Li isotope heterogeneity well beyond analytical uncertainty. As shown in Figure 2a, the $\delta^{7}Li$ exhibits a pattern of three-stage evolution from Zone I to VIII: (1) a sharp increase in Zone I–II, (2) a gradual decrease in Zone III–VI, and (3) a sudden increase in Zone VII–VIII. It is necessary to assess possible processes that might have perturbed the primary $\delta^{7}Li$ of the pegmatite magma and finally have produced this $\delta^{7}Li$ variation pattern.

Internal fluid exsolution

Low-temperature alteration of rock generates secondary minerals with high Li content and heavy δ^7Li[21]. Assimilation of this material may result in an increase in δ^7Li and could alter the chemical composition of rock. Yet, no marked difference can be found with the trace element patterns of the samples from Zone I–II, Zone III–VI and Zone VII–VIII (Figure S1). In addition, the prevailing petrogenetic models of pegmatite have suggested that when the outer zones crystallized the internal system would become closed[3,9]. So it is unlikely that assimilation of exotic materials can change the chemical composition of the rock in the internal zones. Besides of these, the low loss on ignition (LOI) (0.03–0.29%, Table S2) indicates that the samples are fresh and have not been affected by metamorphism. These lines of evidence can exclude the possibility of low-temperature alteration in our samples.

It is also important to consider possible high-temperature fractionation of Li isotope. Magmatic differentiation is incapable of producing notable Li isotopic fractionation[25]. While, diffusion-driven fractionation of Li isotope has been observed in erupted igneous rocks[26] as well as in the country rocks of pegmatite[17]. Nevertheless, our data do not show a systematic variation on δ^7Li that is consistent with the diffusion model from Teng et al.[22]. Thus, high-temperature fractionation can not account for the Li isotopic characteristics of our sample.

Dehydration could produce remarkable Li isotopic fractionation[25,27], and heavier ^{7}Li preferentially enters into the fluids, leading to the residual melts ultimately become isotopically light[21,28-30]. Fluid interaction has been considered as a common process of the internal evolution[4,8,9] and wall-rock alteration[31] of granitic pegmatite. It is noted that the partition coefficient of Cs between fluid and albite ($D_{Cs}^{fluids/Ab}$) is ~250 in the temperature range of 700–800 °C[32]. In agreement with this temperature range, the crystallization temperature of Zone I–III was 700–900 °C as suggested by a fluid inclusion study from Lu et al.[17]. The implication of such large partition coefficient is that Cs would be removed from albite into fluid during fluid exsolution. As shown in Figure 2b, the Cs contents of our sample show decreasing trends from Zone II to I and from Zone II to III, providing evidence that the decreases of δ^7Li from Zone II to I and from Zone II to III have been most possibly caused by fluid exsolution. This can be confirmed by the positive linear correlation

between δ^7Li and Cs (Figure S2). As a consequence, the outward migration of fluid promoted the wall-rock alteration, and the more dramatic change of Cs content ($\Delta Cs_{II–I}$ = 39.65 μg/g) than that of Rb ($\Delta Rb_{II–I}$ = –4.02 μg/g) from Zone II to I is consistent with previous estimates that the migration ratio of Cs is higher than that of Rb[31]. Regarding to the inward migrating fluids, they would participate in the later evolutionary processes. Therefore, these data have revealed that the internal fluid exsolution of the studied pegmatite probably started in Zone III. As a supplement, greisenization of microcline has been observed in Zone III (Figure S3) showing solid evidence for fluid metasomatism.

"Fluid transportation" controls spodumene crystallization

Fluid exsolution could also affect Li content[33]. Experimental study shows that the Li partition coefficient between fluid and melt ($D_{Li}^{fluids/melt}$) ranges from 0 to 5.2 in the pressure range of 200–400 MPa and temperature range of 770–950 °C, and it systematically increases with the increase in mCl^- of fluid[5]. This has been further confirmed by a recent study that the $D_{Li}^{fluids/melt}$ could reach to a maximum of 35±15 in a moderate salinity fluid (mCl^- = 3.0)[34]. According to Lu et al.[17], the mCl^- of fluid in Zone I and III of the studied pegmatite ranges from 5.5 to 12.6, and thus the $D_{Li}^{fluids/melt}$ might be at a high level and probably have exceeded 35±15. In terms of these, it is believable that the decreases of Li from Zone II to I and from Zone II to III (Figure 2c) were produced by fluid exsolution, and as a result, a large amount of Li had been leached from the melt into the fluid.

The gradual decreasing of δ^7Li in Zone IV–VI suggests that the fluid exsolution has lasted during the formation of these zones (Figure 2a), while it is strange that the contents of Cs and Li show increasing trends (Figure 2b–c). The problem here lies in that if the fluid exsolution was in progress the Cs and Li contents of melt would have been reduced. The increases in Cs and Li provide evidence that considerable amounts of Cs and Li had been introduced into the melts. This can be achieved by two processes: (1) crystallization fractionation[35], and (2) unloading from the fluid. As shown in Figure S4, the Cs and Rb contents do not successively decrease with the K/Cs and K/Rb ratios from Zone I to VIII but exhibit multi-stage evolutionary patterns, which are inconsistent with the Rayleigh fractional crystallization model[35]. Moreover, the Cs and Li contents

vary greatly in Zone IV–VI (Figure 2b–c), which might have been more likely caused by fluid interaction rather than by crystallization fractionation. Theoretically, the unloading of Li from fluid into melt requires a decrease in $D_{Li}^{fluids/melt}$. Likewise, the study of the liquid-vapor inclusions in spodumene and quartz of the pegmatite suggests that the mCl^- of fluid has dropped to 0.71–1.68 in Zone IV–VI[17]. According to the model from Webster et al.[5], the $D_{Li}^{fluids/melt}$ is only approximately 0.3–0.7 within this mCl^- range, which is satisfiable for Li unloading. For these reasons, the increasing of Li in Zone IV–VI strongly indicates that considerable amounts of Li might have unloaded from the fluids and concentrated into the melts.

The average Li_2O content of Li-rich pegmatites is close to 0.5 wt.%[36], suggesting that Li mineralization requires a Li content of ~2333 ppm in melt. The partition coefficient of Li between feldspar and felsic melt covers a broad range of 0.09–0.68[37–39], and the calculated Li content of melt for the samples from Zone V–VI is 111–11103 ppm, of which most have exceeded the 2333 ppm. This indicates that the melts in Zone V–VI of the studied pegmatite were capable of Li mineralization. Indeed, a massive crystallization of spodumene has been observed in Zone V–VI (Figure 1).

Here, it is necessary to reconsider the effect of Li unloading on the δ^7Li of melt. Essentially, Li unloading is a chemical diffusion process. Because of the mass difference between Li isotopes, ^6Li diffuses up to 3% more rapidly than ^7Li[40]. Hence, in theory, the Li unloading could also produce a decrease in δ^7Li of melt, which may be confused with the effect of fluid exsolution. It is a fact that a massive crystallization of spodumene occurs in Zone V–VI (Figure 1). Because the crystallization of spodumene could settle large amounts of Li, the Li content of melt would have been reduced correspondingly. However, the Li contents of our sample show an increasing trend from Zone IV to VI successively (Figure 2c). The only explanation for this is that there was a sustainable introducing of Li into the melts, and the imports had exceeded the exports that produced by spodumene crystallization. It is clear that fluid exsolution leaches Li from melt into fluid and the unloading process can result in an increase in Li of melt. Thus, if the fluid exsolution was not in progress, this reaction chain would have inevitably been broken, which could be indicated by a termination of spodumene crystallization or a decrease in Li of melt. As it is not the

case, we are confident that the decreasing of δ^7Li from Zone II to VI was dominantly caused by fluid exoslution, which is important for maintaining the crystallization of spodumene in Zone V–VI.

According to above lines of evidence, it has been revealed that there coexists two critical processes during the internal evolution of the Koktokay No. 3 pegmatite: (1) fluid exsolution and (2) Li unloading. The former facilitates Li enrichment and the later results in spodumene crystallization. These "fluid transportation" processes played the pivotal role in controlling Li mineralization.

The late evolutionary stage of pegmatite magma

The final change of δ^7Li is an increase in Zone VII–VIII (Figure 2a). The Cs and Li contents show gentle decreasing trends and become less varied in these zones (Figure 2b–c), indicating that the Li unloading was not robust and the melt-fluid interaction was not pronounced. The Li fractionation coefficient between pegmatite and muscovite ($\Delta^{Li}_{pegmatite–Ms} = \delta^7Li_{pegmatite} - \delta^7Li_{Ms}$) is ~1.8‰[24]. As such, the crystallization of muscovite in Zone VII (Figure 1) is the most likely cause of the increase in δ^7Li of albite. With the crystallization of muscovite, the Li content in fluid increased, leading to the crystallization of lepidolite in Zone VIII. This is consistent with the field observations and is the best explanation for the decreasing of Li in Zone VII–VIII (Figure 2c).

Global Li mineralized granitic pegmatites

In summary of our study, it is appealing that during the internal evolution of pegmatite magma fluid exsolution causes the decreasing in δ^7Li of melt and Li unloading leads to the increasing in Li of melt. As such, the "fluid transportation" can be indicated by a negative correlation between δ^7Li value and Li content (Figure 3a). Here, we have collected Li isotopic data of global granites and Li mineralized pegmatites (DR1). The results show that there is also a negative correlation between δ^7Li and Li both in the whole rock and separated mineral samples of pegmatite (Figure 3b), providing compelling evidence that "fluid transportation" is the key mechanism responsible for Li mineralization in granitic pegmatite. This finding is of great significance for Li metal deposit modeling and mineral exploration, implying that the intensity of fluid action in pegmatite

Li deposits can be used as a new indicator for evaluation the degree of mineralization and prediction of ore prospecting.

Methods

In this study, the samples of 8 zones of the Koktokay No. 3 pegmatite were collected in the mined open pit (Figure 1), and each sample is more than 5 kg. The samples were crashed to 80 mesh, and albite minerals were separated under a binocular microscope. The pure albite mineral grains were then crashed to 200–400 mesh. Major element, trace element and Li isotope compositions were measured at the State Key Laboratory of Ore Deposit Geochemistry, Institute of Geochemistry, Chinese Academy of Sciences (IGCAS).

Major and trace elements. Major elements of samples were determined by using a wavelength-dispersive X-ray fluorescence spectrometry with analytical deviations less than 1%. Loss on ignition was obtained through heating a 1 g sample powder at 1100 °C for 1 h. The international standards BHVO-2 and AGV-2 were applied to control analytical quality (Table S4). Trace elements were analyzed by using an inductively coupled plasma mass spectrometry (ICP-MS). The samples were digested by HF + $HClO_4$ acid in bombs. The international standard GBPG-1, the Chinese National standard GSR-1 and the laboratory standard W-2 were applied to control analytical quality (Table S5). Sample preparations, instrument operating conditions and calibration procedures are applied by Qi and Grégoire[41].

Li isotopes. The procedure for sample preparation and chemical separation followed the published articles[42–46]. Approximately 100 mg of each rock powder was digested in Teflon® beakers with 3 ml concentrated HF and 0.5 ml 6M HNO_3 for 24 h on a hot plate at 130 °C. Then, the residue was re-digested with 1ml 6M HCl for 24 h on a hot plate at 130 °C. After evaporation of the solution, the residue was re-dissolved and dried down three times in 6M HNO_3 to remove fluorides completely. Finally, the samples were put on the hot plate and make sure all the solution was evaporated. The cation-exchange resin (BioRad® AG50W-X8, 200–400 mesh) was cleaned by repeated flushing with 5 ml of 6 M HCl and 5 ml of deionized water, then with 5 ml of 6 M HNO_3 and 5 ml of deionized water. A conditioning agent (5M HNO_3 : methanol = 1 : 4) was prepared before loading of a sample. At first, 1.5 ml of the conditioning agent was loaded to moist the column. Then, 0.18 ml 5M HNO_3 was added into the beakers to make samples dissolved (not on hot plate),

followed by added 0.72 ml 100% methanol into the beakers. The samples were quickly put into the column, and the entire protocol used for Li separation is listed in Table S6. All separations were monitored with ICP-MS analysis to guarantee both high Li yield (> 99.8% recovery) and low Na/Li ratio (Na/Li < 0.5). The total procedural blank was less than 0.03 ng of Li, indicating that the influence of the chemical separation procedures on the Li in the sample was negligible (< 0.1%). The collected Lithium sample solution was evaporated until dry in a clean evaporator and then dissolved in 5% HNO_3, in preparation for the MC-ICP-MS method. Lithium isotopic compositions were measured on a Thermo Scientific Neptune Plus MC-ICP-MS, with ^{7}Li and ^{6}Li measured simultaneously in separate Faraday cups. Each sample analysis is bracketed by measurements of the L-SVEC[47] (a Li carbonate standard) having a similar Li concentration, and the results are calculated as $\delta^{7}Li = \{[(^{7}Li/^{6}Li)_{sample}/(^{7}Li/^{6}Li)_{L\text{-}SVEC}] - 1\} \times 1000$. Two Li standards (Li-UMD-1 and IRMM-016) are routinely analyzed during the course of each analytical session. Our average $\delta^{7}Li$ results are +54.6±0.8‰ (2σ, n = 8) for UMD-1, and +0.1±0.3‰ (2σ, n = 8) for IRMM-016. Five international reference rock materials (JG-2, AGV-2, BHVO-2, BCR-2 and G-2) were measured to monitor the reproducibility and accuracy of the analytical procedure. Repeat analysis of these rock standards yielded 0.41±0.38‰ (2SD, n = 7) for JG-2, 8.10±0.57‰ (2SD, n = 7) for AGV-2, 4.54±0.37‰ (2SD, n = 7) for BHVO-2, 2.97±0.34‰ (2SD, n = 7) for BCR-2 and –0.02±0.41‰ (2SD, n = 7) for G-2, which are consistent with previously published results (see *Supplementary Materials*). The data are presented in *Data Repository File DR1*.

References

1. Kesler, S.E., Gruber, P.W., Medina, P.A., Keoleian, G.A., Everson, M.P., & Wallington, T.J. Global lithium resources: Relative importance of pegmatite, brine and other deposits. *Ore Geology Reviews* **48**, 55–69 (2012).
2. Černý, P., London, D. & Novak, M. Granitic pegmatites as reflections of their sources. *Elements* **8**, 257–261 (2012).
3. London, D. A petrologic assessment of internal zonation in granitic pegmatites. *Lithos* **184-187**, 74–104 (2014).
4. London, D. Ore-forming processes within granitic pegmatites. *Ore Geology Reviews* **101**, 349–383 (2018).

5. Webster, J.D., Holloway, J.R. & Hervig, R.L. Partitioning of lithophile trace elements between H_2O and $H_2O + CO_2$ fluids and topaz rhyolite melt. *Economic Geology* **84**, 116–134 (1989).
6. Shearer, C.K., Papike, J.J. & Jolliff, B.L. Petrogenetic links among granites and pegmatites in the Harney Peak rare-element granite-pegmatite system, Black Hills, South Dakota. *Canadian Mineralogist*, **30**, 785–809 (1992).
7. Veksler, I.V., Thomas, R. & Schmidt, C. Experimental evidence of three coexisting immiscible fluids in synthetic granitic pegmatite. *American Mineralogist*, **87**, 775–779 (2002).
8. Thomas, R. & Davidson, P. Revisiting complete miscibility between silicate melts and hydrous fluids, and the extreme enrichment of some elements in the supercritical state-Consequences for the formation of pegmatites and ore deposits. *Ore Geology Reviews* **72**, 1088–1101 (2016).
9. Jahns, R.H. & Burnham, C.W. Experimental studies of pegmatite genesis: I. A model for the derivation and crystallization of granitic pegmatites. *Economic Geology* **64**, 843–864 (1969).
10. London, D. The application of experimental petrology to the genesis and crystallization of granitic pegmatites. *The Canadian Mineralogist* **30**, 499–540 (1992).
11. Maneta, V. & Baker, D.R. Exploring the effect of lithium on pegmatitic textures: An experimental study. *American Mineralogist* **99**, 1383–1403 (2014).
12. London, D. & Morgan G.B. Experimental Crystallization of the Macusani Obsidian, with Applications to Lithium-rich Granitic Pegmatites. *Journal of Petrology* **58(5)**, 1005–1030 (2017).
13. Sirbescu, M.L.C., Schmidt, C., Veksler, I.V., Whittington, A.G. & Wilke, M. Experimental Crystallization of Undercooled Felsic Liquids: Generation of Pegmatitic Texture. *Journal of Petrology* **58(3)**, 539–568 (2017).
14. Devineau, K., Champallier, R. & Pichavant, M. Dynamic Crystallization of a Haplogranitic Melt: Application to Pegmatites. *Journal of Petrology* **61(5)**, 1–25 (2020).
15. London, D., Pegmatites. *Canadian Mineralogist Special Publication,* **10**, 1–347 (2008).
16. Liu, C. & Zhang, H. The lanthanide tetrad effect in apatite from the Altay No. 3 pegmatite, Xingjiang, China: an intrinsic feature of the pegmatite magma. *Chemical Geology* **214**,

61–77 (2005).

17. Lu, H., Wand, Z. & Li, Y. Magma-fluid transition and the genesis of pegmatite dike No.3, Altay, Xinjiang, Northwest China. *Chinese Journal of Geochemistry* **16**, 43–52 (1997).
18. London, D., Morgan VI, G.B. & Hervig, R.L. Vapor-undersaturated experiments in the system macusanite + H_2O at 200 MPa, and the internal differentiation of granitic pegmatites. *Contributions to Mineralogy and Petrology* **102**, 1–17 (1989).
19. Thomas, A.V. & Spooner, E.T.C. The volatile geochemistry of magmatic H_2O-CO_2 fluid inclusions from the Tanco zoned granitic pegmatite, southeastern Manitoba, Canada. *Geochimica et Cosmochimica Acta* **56**, 49–65 (1992).
20. Cooper, D.G. The geology of the Bikita pegmatite. In: Haughton, S.H. (Ed.), The Geology of Some Ore Deposits of Southern Africa. *Geological Survey of South Africa, Johannesburg* **2**, 441–461 (1964).
21. Chan, L. H., Edmond, J. M. & Thompson, G. A lithium isotope study of hot springs and metabasalts from mid-ocean ridge hydrothermal systems. *Journal of Geophysical Research* **98(B6)**, 9653–9659 (1993).
22. Teng, F., McDonough, W.F., Rudnick, R.L. & Walker, R.J., 2006, Diffusion-driven extreme lithium isotopic fractionation in country rocks of the Tin Mountain pegmatite. Earth and Planetary Science Letters, v. 243, p. 701–710.
23. Elliott, T., Thomas, A., Jeffcoate, A. & Niu, Y. Lithium isotope evidence for subduction-enriched mantle in the source of mid-ocean-ridge basalts. *Nature* **443**, 565–568 (2006).
24. Chen, B., Huang, C. & Zhao, H. Lithium and Nd isotopic constraints on the origin of Li-poor pegmatite with implications for Li mineralization. *Chemical Geology* **551**, 119769 (2020).
25. Tomascak, P. B., Tera, F., Helz, R. T. & Walker, R. J. The absence of lithium isotope fractionation during basalt differentiation: new measurements by multicollector sector ICP-MS. *Geochimica et Cosmochimica Acta* **63**, 907–910 (1999).
26. Li, J., Huang, X., Wei, G., Liu, Y., Ma, J., Han, L. & He, P. Lithium isotope fractionation during magmatic differentiation and hydrothermal processes in rare-metal granites. *Geochimica et Cosmochimica Acta* **240**, 64–79 (2018).
27. Lundstrom, C. C., Chaussidon, M., Hsui, A. T., Kelemen, P. & Zimmerman, M. Observations

of Li isotopic variations in the Trinity Ophiolite: evidence for isotopic fractionation by diffusion during mantle melting. *Geochimica et Cosmochimica Acta* **69**, 735–751 (2005).

28. Magna, T., Novák, M., Cempírek, J., Janoušek, V., Ullmann, C. & Wiechert, U. Crystallographic control on lithium isotope fractionation in Archean to Cenozoic lithium-cesium-tantalum pegmatites. *Geology* **44**, 656–658 (2016).
29. Zack, T., Tomascak, P. B., Rudnick, R. L., Dalpé, C. & McDonough, W. F. Extremely light Li in orogenic eclogites: the role of isotope fractionation during dehydration in subducted oceanic crust. *Earth and Planetary Science Letters* **208**, 279–290 (2003).
30. Maloney, J.S., Nabelek, P.I., Sirbescu, M.C. & Halama, R. Lithium and its isotopes in tourmaline as indicators of the crystallization process in the San Diego County pegmatites, California, USA. *European Journal of Mineralogy* **20(5)**, 905–916 (2008).
31. Zhao, J., Zhang, H., Tang, Y. & Lü, Z. Ore-forming elements diffusion and distribution in the altered host rock surrounding the Koktokay No. 3 pegmatite in the Chinese Altay. *Acta Geochim* **36**, 151–165 (2017).
32. Carron, J.P. & Lagache, M. Étude expérimentale du fractionnement des éléments Rb, Cs, Sr, et Ba entre feldspaths alcalins, solutions hydrothermales et liquides silicatés dans le système Q.Ab.Or.H2O à 2 kbar entere 700 et 800 °C. *Bulletine de Minéralogie* **103**, 571–578 (1980).
33. Wunder, B., Meixner, A., Romer, R.L., Feenstra, A., Schettler, G. & Heinrich, W. Lithium isotope fractionation between Li-bearing staurolite, Li-mica and aqueous fluids: an experimental study. *Chemical Geology* **238**, 277–290 (2007).
34. Zajacz, Z., Halter, W.E., Pettke, T. & Guillong, M. Determination of fluid/melt partition coefficients by LA-ICPMS analysis of co-existing fluid and silicate melt inclusions: Controls on element partitioning. *Geochimica et Cosmochimica Acta* **72**, 2169–2197 (2008).
35. Hulsbosch, N., Hertogen, J., Dewaele, S., André, L. & Muchez, P. Alkali metal and rare earth element evolution of rock-forming minerals from the Gatumba area pegmatites (Rwanda): Quantitative assessment of crystal-melt fractionation in the regional zonation of pegmatite groups. *Geochimica et Cosmochimica Acta* **132**, 349–374 (2014).
36. Stewart, D.B. Petrogenesis of lithium-rich pegmatites. *American Mineralogist* **63**, 970–980 (1978).
37. Aigner-Torres, M., Blundy, J., Ulmer, P. & Pettke, T. Laser ablation ICPMS study of trace

element partitioning between plagioclase and basaltic melts: an experimental approach. *Contributions to Mineralogy and Petrology* **153**, 647–667 (2007).

38. Bindeman, I.N. & Davis, A.M. Trace element partitioning between plagioclase and melt: investigation of dopant influence on partition behaviour. *Geochimica et Cosmochimica Acta* **64**, 2863–2878 (2000).
39. Sun, C., Graff, M. & Liang, Y. Trace element partitioning between plagioclase and silicate melt: The importance of temperature and plagioclase composition, with implications for terrestrial and lunar magmatism. G*eochimica et Cosmochimica Acta* **206**, 273–295 (2017).
40. Richter, F.M., Davis, A.M., DePaolo, D.J. & Watson, E.B. Isotope fractionation by chemical diffusion between molten basalt and rhyolite. *Geochimica et Cosmochimica Acta* **67**, 3905–3923 (2003).
41. Qi, L. & Grégoire, D.C. Determination of Trace Elements in Twenty Six Chinese Geochemistry Reference Materials by Inductively Coupled Plasma-Mass Spectrometry. *Geostandards Newsletter* **24**, 51–63 (2000).
42. Magna, T., Wiechert, U.H. & Halliday, A.N. Low-blank isotope ratio measurement of small samples of lithium using multiple-collector ICPMS. *International Journal of Mass Spectrometry* **239**, 67–76 (2004).
43. Li, J., Huang, X., Wei, G., Liu, Y., Ma, J., Han, L. & He, P. Lithium isotope fractionation during magmatic differentiation and hydrothermal processes in rare-metal granites. *Geochimica et Cosmochimica Acta* **240**, 64–79 (2018).
44. Liu, X.M., Rudnick, R.L., Hier-Majumder, S. & Sirbescu, M.L.C. Processes controlling lithium isotopic distribution in contact aureoles: A case study of the Florence County pegmatites, Wisconsin. *Geochemistry, Geophysics, Geosystems* **11**, Q08014 (2010).
45. Lin, J., Liu, Y., Hu, Z., Yang, L., Chen, K., Chen, H, Zong, K. & Gao, S. Accurate determination of lithium isotope ratios by MC-ICP-MS without strict matrix-matching by using a novel washing method. *Journal of Analytical Atomic Spectrometry* **31**, 390–397 (2016).
46. Jeffcoate, A.B., Elliott, T., Thomas, A. & Bouman C. Precise/small sample size determinations of lithium isotopic compositions of geological reference materials and modern seawater by MC-ICP-MS. *Geostandards and Geoanalytical Research* **28**, 161–172

(2004).

47. Flesch, G.D., Anderson Jr., A.R. & Svec, H.J. A secondary isotopic standard for $^{6}Li/^{7}Li$ determinations. *International Journal of Mass Spectrometry and Ion Physics* **12**, 265–272 (1973).

Acknowledgements

The research leading to these results has received funding from the National Natural Science Foundation of China (Grant No. 91962222 and Grant No. 42062004) and Department of science and technology of Ningxia Hui Autonomous Region (Grant No. 2019BEB04016).

Author contributions

X.Z. conceived the research idea. X.Z. and H.Z. funded the research. X.Z., H.Z., Y.T., Z.L., S.G. and M.W. performed the fieldwork and collected the samples. X.Z. analysed the data and wrote the manuscript with contributions from all other co-authors.

Additional Information

Competing interests. The authors declare no competing interests.

Data availability. All data associated with this work are available in *Supplementary Materials* and *Data Repository File DR1*.

Figure legends

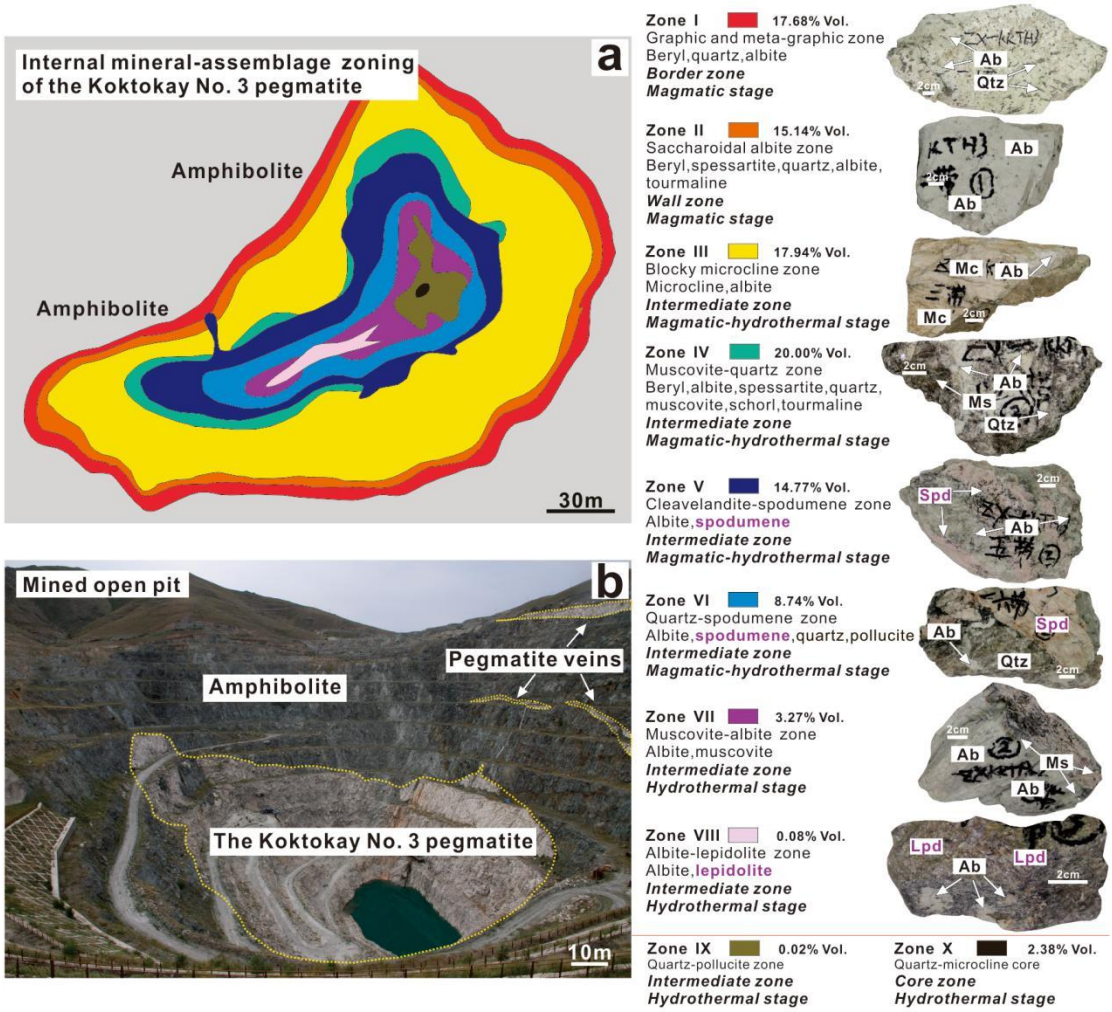

Figure 1. Geological maps of the Koktokay No. 3 pegmatite showing (**a**) the internal mineral-assemblage zoning and (**b**) field occurrence of the mined open pit (*Ab*: albite, *Qtz*: quartz, *Mc*: microcline, *Ms*: Muscovite, *Spd*: spodumene, *Lpd*: lepidolite).

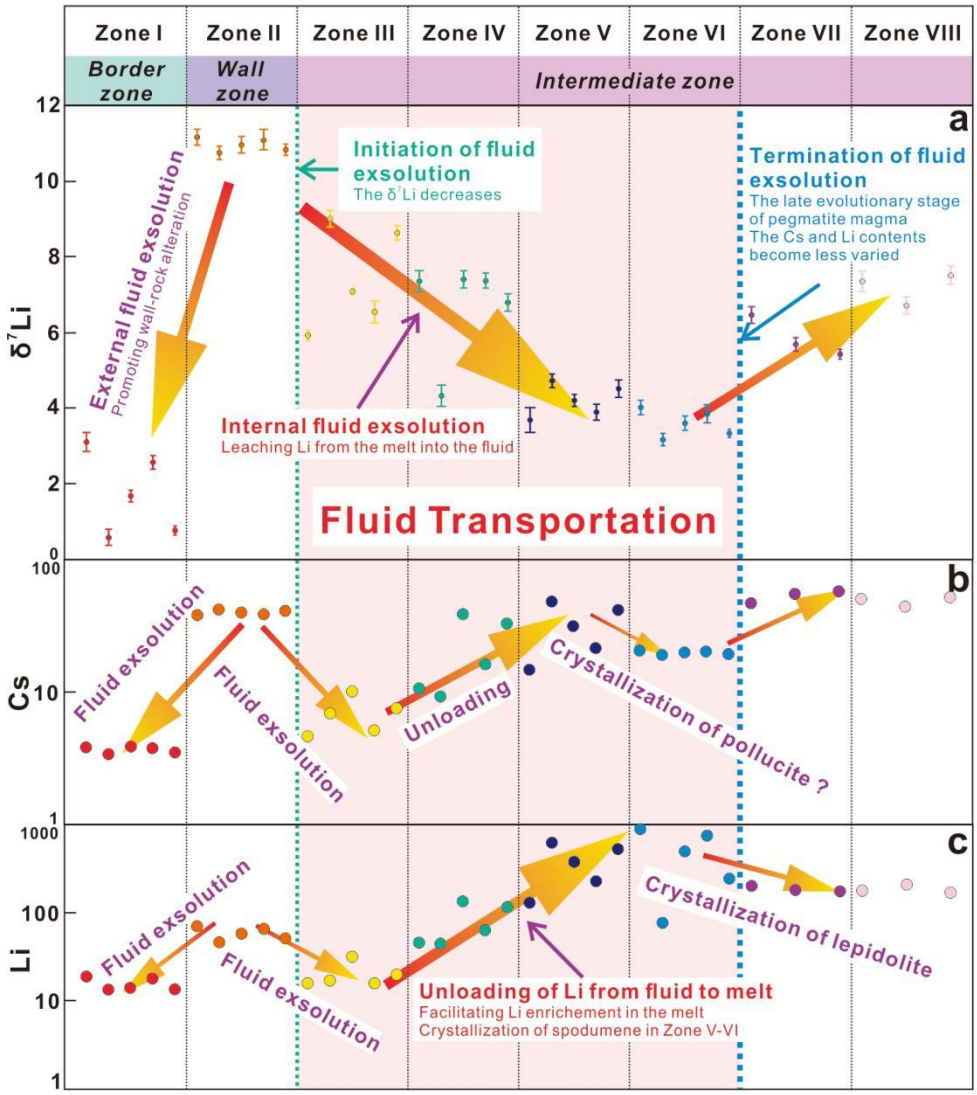

Figure 2. Isotopic and elemental compositions of samples. **a** Variation on Li isotope of the samples of Zone I–VIII showing a decrease in Zone II–I, a decrease in Zone III–VI, and an increase in Zone VII–VIII. **b** Variation on Cs content of the samples of Zone I–VIII showing a decrease in Zone II–I, a decrease in Zone II–III, an increase in Zone IV–V, a decrease in Zone V–VI and an increase in VII–VIII. **c** Variation on Li content of the samples of Zone I–VIII showing a decrease in Zone II–I, a decrease in Zone II–III, an increase in Zone IV–VI and a decrease in Zone VII–VIII. The decreasing of δ^7Li, Cs and Li from Zone II to I indicates the external fluid exsolution. The decreasing of δ^7Li, Cs and Li in Zone II–III indicates the initiation of the internal fluid exsolution which had leached Li from the melt into the fluid. The decreasing of δ^7Li in Zone IV–VI indicates that fluid exsolution had lasted during the formation of these

zones. The increasing of Li in Zone IV–VI indicates that a large amount Li had unloaded from the fluid and concentrated into the melt, and these processes had facilitated the crystallization of spodumene in Zone V–VI. The change of δ^7Li between Zone VI and VII may be a sign of the termination of fluid exsolution.

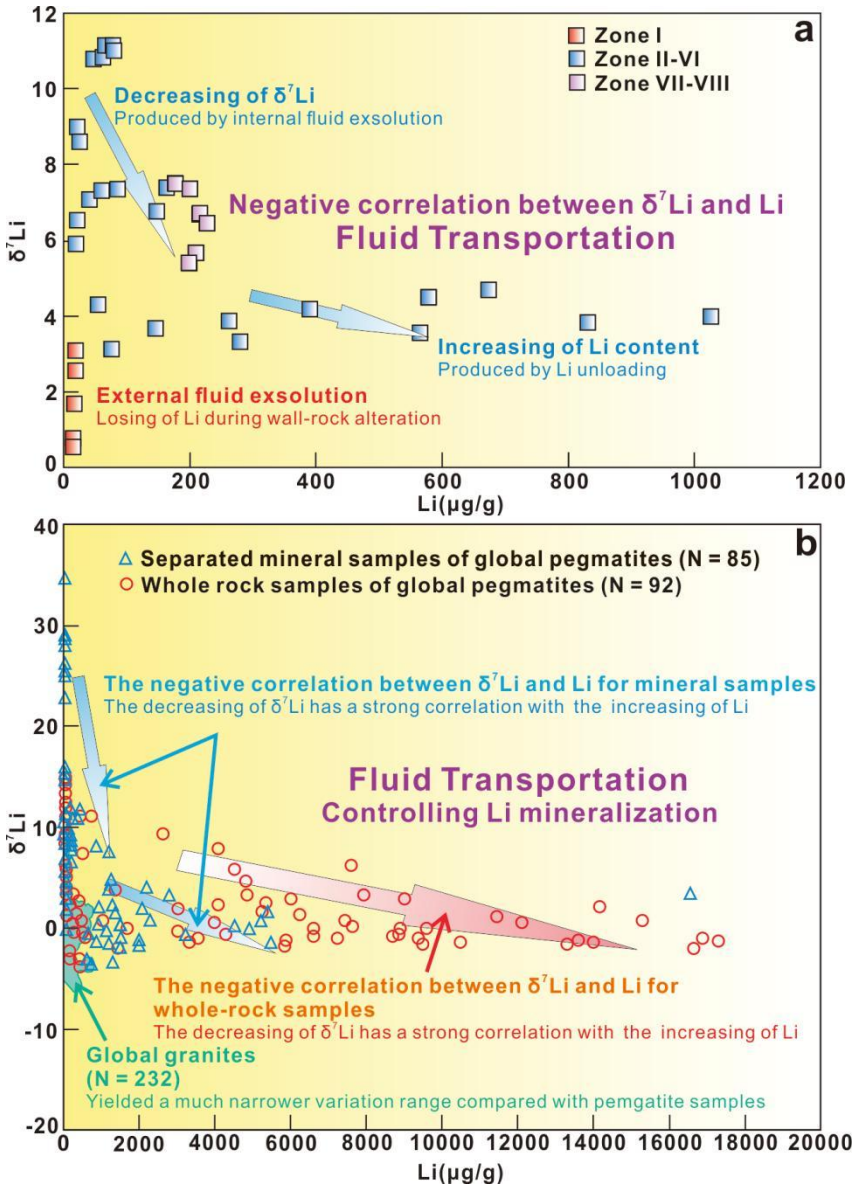

Figure 3. Li vs. δ^7Li diagrams of our samples (**a**) and of global granite and pegmatite samples (**b**) showing that the decreasing of δ^7Li has a strong correlation with the increasing of Li for both of the pegmatite separated mineral and whole rock samples, indicating that "fluid transportation" is the key mechanism controlling Li mineralization in granitic pegmatite (The data are given in *Data Repository File DR1*).

Supplementary Files

This is a list of supplementary files associated with this preprint. Click to download.

- DataRepositoryFileDR1.xls
- SupplementaryMaterials.pdf